

Mutant presenilins of Alzheimer's disease increase production of 42-residue amyloid β -protein in both transfected cells and transgenic mice

MARTIN CITRON¹, DAVID WESTAWAY², WEIMING XIA¹, GEORGE CARLSON³, THEKLA DIEHL¹, GEORGES LEVESQUE², KELLY JOHNSON-WOOD⁴, MICHAEL LEE⁴, PETER SEUBERT⁴, ANGELA DAVIS³, DORA KHOLODENKO⁴, RUTH MOTTER⁴, ROBIN SHERRINGTON², BILLIE PERRY³, HONG YAO², ROBERT STROME², IVAN LIEBERBURG⁴, JOHANNA ROMMENS², SOYEON KIM⁵, DALE SCHENK⁴, PAUL FRASER², PETER ST GEORGE HYSLOP² & DENNIS J. SELKOE¹

¹Center for Neurologic Diseases, Brigham and Women's Hospital and Harvard Medical School, 221 Longwood Avenue, Boston, Massachusetts 02115, USA

²Centre for Research into Neurodegenerative Disease, Departments of Medicine (Neurology), Medical Biophysics, Medical and Molecular Genetics and Pathology, University of Toronto, 6 Queen's Park Crescent, Toronto, Ontario, Canada M5S 1A8

³McLaughlin Research Institute, 1520 23rd Street South, Great Falls, Montana 59409, USA

⁴Athena Neurosciences Inc., 800F Gateway Boulevard, South San Francisco, California 94080, USA

⁵Department of Biostatistics, Harvard School of Public Health, Boston, Massachusetts 02115, USA

Correspondence should be addressed to M.C. or D.J.S.

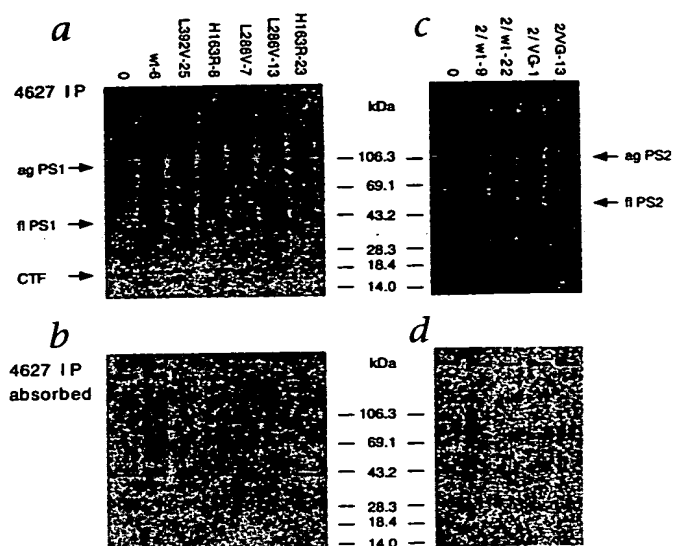
The mechanism by which mutations in the presenilin (*PS*) genes cause the most aggressive form of early-onset Alzheimer's disease (AD) is unknown, but fibroblasts from mutation carriers secrete increased levels of the amyloidogenic $A\beta_{42}$ peptide, the main component of AD plaques. We established transfected cell and transgenic mouse models that coexpress human *PS* and amyloid β -protein precursor (*APP*) genes and analyzed quantitatively the effects of *PS* expression on *APP* processing. In both models, expression of wild-type *PS* genes did not alter *APP* levels, α - and β -secretase activity and $A\beta$ production. In the transfected cells, *PS1* and *PS2* mutations caused a highly significant increase in $A\beta_{42}$ secretion in all mutant clones. Likewise, mutant but not wild-type *PS1* transgenic mice showed significant overproduction of $A\beta_{42}$ in the brain, and this effect was detectable as early as 2–4 months of age. Different *PS* mutations had differential effects on $A\beta$ generation. The extent of $A\beta_{42}$ increase did not correlate with presenilin expression levels. Our data demonstrate that the presenilin mutations cause a dominant gain of function and may induce AD by enhancing $A\beta_{42}$ production, thus promoting cerebral β -amyloidosis.

The mechanism by which presenilin mutations cause the most malignant form of Alzheimer's disease (AD) is currently unknown. Because several lines of evidence strongly support the conclusion that progressive cerebral deposition of amyloid β -protein ($A\beta$) is a seminal event in AD pathogenesis (reviewed in ref. 1), it has been hypothesized that all known early-onset familial Alzheimer's disease (FAD) mutations act to foster $A\beta$ deposition, particularly of the highly amyloidogenic² 42-residue form. A recent study³ demonstrated that skin fibroblasts cultured from *PS1* and *PS2* mutation carriers indeed secrete significantly elevated amounts of $A\beta_{42}$, suggesting that the pathogenic effect of the presenilin mutations may be at the level of $A\beta_{42}$ production. Here we confirm and extend these initial findings in transfected human cells in which the sole variable is the introduction of *PS1* and *PS2* genes, and any other host-derived factors are eliminated⁴. Moreover, we directly show that the same effect occurs under *in vivo* conditions, that is, in the brains of mice expressing both *APP* and mutant *PS1* transgenes.

Transfected cell lines

In order to obtain stable constitutive *APP*/presenilin double-

transfectants, 293 human embryonic kidney cells stably expressing *APP₆₉₅*, carrying the Swedish *APP* mutation⁵ were transfected with *PS1* or *PS2* cDNA constructs. The Swedish mutation makes *APP* a better substrate for β -secretase⁶ and thus increases the production of both $A\beta_{40}$ and $A\beta_{42}$ (ref. 3). This particular cell line was chosen for the *PS* transfections because its high total $A\beta$ secretion allows an accurate quantification of $A\beta_{42}$ by our sandwich enzyme-linked immunosorbent assay (ELISA). In addition, the availability of an antibody specific for the β -cleaved form of *APP*, of the Swedish variant allows a direct analysis of β -secretase cleavage^{7,8}. The presenilin expression plasmids contain the cDNA of *PS1*, *PS2* or mutant forms of these genes under transcriptional control of the CMV promoter. We selected stable lines of wild-type *PS1* and the *PS1* mutants H163R, L286V and L392V and wild-type *PS2* and the *PS* mutant N141I (Volga German). Figure 1a shows *PS1* expression of several double-transfected cell lines, as detected by immunoprecipitation of cell lysates with the carboxy-terminal presenilin antibody 4627 (M.B. Podlisny *et al.*, manuscript submitted). All lines show an increase in the circa 18-kDa C-terminal *PS1* endoproteolytic fragment⁹, compared with that of nontransfected cells. In addition, the high express-



ing lines wt-6, L392V-25, H163R-8 and L286V-7, but not the low-level expressors H163R-23 and L286V-13, show the broad full-length PS1 monomer band running slightly below 43 kDa and the characteristic higher molecular weight aggregates that have been previously described¹⁰ (Fig. 1a). These bands are specific, as demonstrated by peptide absorption (Fig. 1b). The results are consistent with the data of Thinakaran *et al.*⁹ and M.B. Podlisny *et al.* (manuscript submitted), who demonstrated that untransfected cells and low-level PS1 overexpressing cells show only the stable N- and C-terminal fragments, whereas full-length PS1 becomes detectable only when substantial overexpression is achieved. All cell lines shown in Fig. 1 have had stable presenilin

Fig. 1 a, Cells stably transfected with APP alone (0) or with PS1 wild-type (wt) or one of the indicated PS1 mutants were labeled for 150 min. Extracts were immunoprecipitated with the C-terminal PS antibody 4627, which detects monomeric full-length PS1 (fl PS1), as a broad, fuzzy band just beneath the 43-kDa background band, PS1 aggregates (ag PS1) and C-terminal proteolytic fragments (CTF). The broad band running at about 100 kDa was identified as PS1 aggregates because the size changes as expected when parts of the monomeric molecule are recombinantly deleted. b, Aliquots of the same extracts were immunoprecipitated with 4627 preabsorbed with the immunogenic peptide. The fuzzy band just below 43 kDa is removed. c, Cells stably transfected with APP alone (0) or with PS2 wild-type (2/wt) or PS2 Volga German mutant (2/VG) were precipitated with 4627. This antibody has a higher affinity for PS1 than for PS2. Therefore the PS2 full-length bands are rather faint. One cannot expect to detect C-terminal PS2 proteolytic fragments after the short labeling used here. d, Precipitation as in (c) after preabsorption of antibody 4627.

levels for several months. Cell lines transfected with PS2 were analyzed in the same way, since 4627 also precipitates PS2 (M.B. Podlisny *et al.*, manuscript submitted). In all four lines, a broad fuzzy band with an apparent molecular weight of about 50 kDa which is absorbable and not detectable in untransfected cells, indicates stable PS2 expression (Fig. 1, c and d). In addition, the expected higher molecular weight aggregates¹⁰ are observed.

We analyzed the effects of PS mutations on APP processing using all of the cell lines shown in Fig. 1. No qualitative change in the immunoprecipitation pattern of full-length APP or its C-terminal fragments were observed when steady-state levels of APP in nontransfected, wild-type-transfected, and mutant PS1 and PS2-transfected lines were analyzed with the C-terminal APP antibody C7 (ref. 11). In addition, no qualitative differences among the different lines were observed in the steady-state immunoprecipitation patterns of α -APP, [antibody 1736 (ref. 12)], β -APP, [antibody 192sw (ref. 7)], and $A\beta_{1-42}$ and $A\beta_{42}$, [antibodies 1282 (ref. 13) and 21F12 (ref. 14), respectively] (not shown). To quantify any PS1-induced changes in the steady-state levels of full-length APP, α -APP, and β -APP, eight immunoprecipitation experiments were carried out on different days and analyzed by phosphor imaging. The results of each experiment were normalized to those in the untransfected line (Table 1). No significant differences in the steady-state levels of full-length APP, α -APP, and β -APP, were detected between all PS1-transfected cells and untransfected cells, or between untransfected plus PS1 wild-type-transfected cells and all PS1 mutant-transfected cells. For PS2, significant differences were found in the steady-state levels of full-length APP, α -APP, and β -APP, between untransfected and PS2VG-transfected cells. These data indicate that the pathological effect of the presenilin mutations is unlikely to involve A metabolites other than $A\beta$.

To quantify changes in $A\beta$ production, media from all stable lines were conditioned for 21 hours, and we assayed total $A\beta$ and $A\beta_{1-42}$ by highly specific sandwich ELISAs (Table 1). These ELISAs detect only $A\beta$ starting at Asp1. Four sets of experiments with two sister dishes of each clone were carried out for the PS1 lines and five sets of experiments with two sister dishes of each clone were carried out for the PS2 lines. For PS1, a significant increase of total $A\beta$ compared with that of nontransfected cells was observed only for the lines H163R-8 and L286V-13 but not

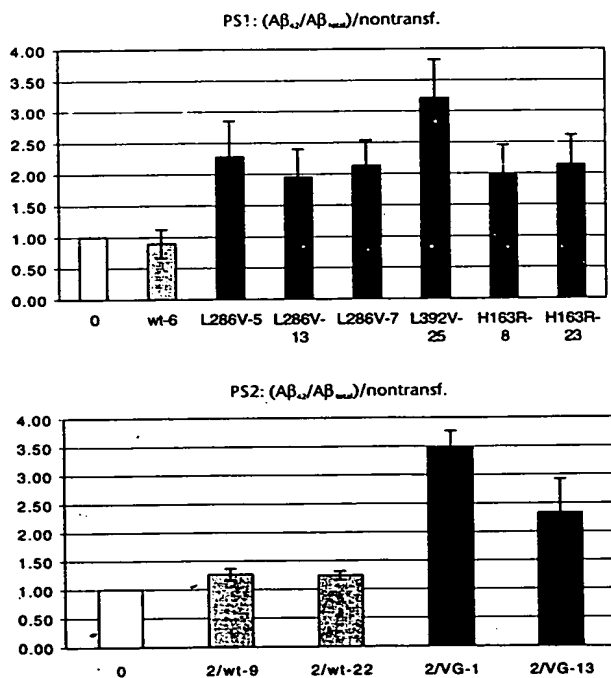


Fig. 2 The $A\beta_{42}/A\beta_{total}$ ratio normalized to that in nontransfected cells (Table 1) is plotted for all clones analyzed in this study. Data shown are means. Error bars indicate the standard deviations.

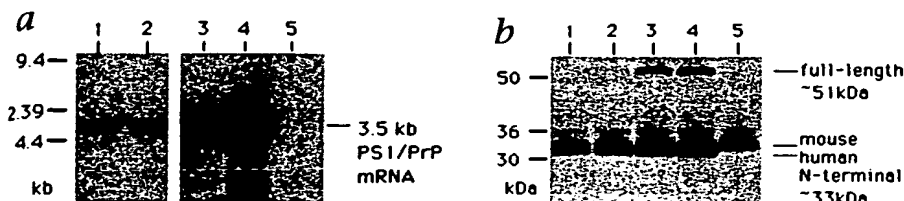


Fig. 3 *a*, Northern blot of total RNA (10 µg per lane) from the brains of transgenic and control mice using a human-specific PS1 cDNA hybridization probe. Lane 1: L286V, line Tg198; lane 2: PS1 wild-type, line Tg195; lane 3: M146L, line Tg1; lane 4: M146L, line Tg29; lane 5: non-Tg control. All RNA samples were separated by electrophoresis on the same gel, transferred and hybridized in parallel. The positions of the transgene-encoded mRNA, comprising PS1 coding sequences and PrP untranslated sequences, are indicated. Exposure time, 16 h. *b*, Western blot of brain lysates from the same mice as in *a*, using the N-terminal PS1 antibody, Ab14. Lanes as in *a*. Positions of the transgenic human PS1 holoprotein ("full-length") and of the endogenous mouse and transgenic human N-terminal endoproteolytic fragments are indicated.

other clones of the same mutations. Compared with nontransfected cells, the levels of total Aβ were not elevated by transfection with PS2 wild-type, but the PS2VG mutant transfectants

showed a two- to threefold increase in total Aβ that was highly significant ($P = 0.0001$). Aβ₁₋₄₂ levels were significantly elevated (~1.5- to 3-fold) compared with nontransfected cells for all PS1 mutant clones ($P < 0.003$ for each comparison), including the L286V mutation that showed a nonsignificant Aβ₁₋₄₂ elevation in the fibroblast study¹. Aβ₁₋₄₂ levels were increased more than five times in the PS2VG mutant clones. No Aβ₁₋₄₂ elevation was found in the PS1 wild-type and PS2 wild-type clones. These data indicate that mutations in both presenilin genes consistently increase Aβ₁₋₄₂ production (Table 1). This effect was clearly confirmed when we calculated the ratio of Aβ₁₋₄₂/Aβ_{total}, a measure of the relative utilization of the 42-cleavage pathway that eliminates differences in total Aβ production, APP expression, cell number and so on. Compared with the nontransfected cells, all the mutant PS1 clones as well as the PS2VG mutant showed a highly significant increase in this ratio ($P = 0.0001$ for each pairwise comparison). Furthermore, different clones of the same PS1 mutant showed an almost identical Aβ₁₋₄₂/Aβ_{total} ratio, although the absolute Aβ_{total} and Aβ₁₋₄₂ levels were different and the PS1 expression levels vary dramatically (Fig. 1). The extent of the Aβ₁₋₄₂/Aβ_{total} ratio showed a crude inverse correlation with mean age of disease onset for the three different PS1 mutations we examined.

Transgenic mice

We bred transgenic mice bearing a human wild-type APP₆₉₅ gene with mice bearing different human PS1 transgenes to produce offspring expressing wild-type human APP₆₉₅ alone (single-transgenic mice) or both wild-type APP₆₉₅ and either mutant or wild-type human PS1 (double-transgenic mice). This strategy was chosen because endogenous mouse APP is not associated with Aβ deposition under physiological or naturally occurring pathological conditions. In addition, use of the same promoter element for both transgenes offers the advantage that both transgenes are likely to be expressed in adequate quantities in the same cells. Because all parental lines were produced using the same inbred FVB/N mice, the only difference between double- and single-transgenic animals is the presence or absence of the human PS1 transgene and any associated insertional mutation.

Transgenic mice overexpressing wild-type human APP₆₉₅ were constructed using the prion protein (PrP)-derived cos.Tet expression vector, in which the human APP₆₉₅ cDNA was cloned downstream of the promoter, a 5' UTR exon, and an intron all derived from the Syrian hamster PrP gene¹⁵. The cos.Tet vector was chosen because it induces position-independent expression of the transgene in many CNS neurons and some astrocytes^{16,17} and has been successfully used to create transgenic mice over-expressing human APP₆₉₅ (ref. 18). The PS1 cDNAs were derived from the clone CC33, which contains a full-length PS1 open reading frame (ORF) including the alternatively spliced residues 324–335 in exon 4 and residues 1018–1116 in exon 9 (ref. 19, 20). Two different mutant transgenes were created, namely, the M146L and

Table 1 Effect of presenilin proteins on APP processing in transfected cells

<i>a</i>				
Line	fl APP/nt	α-APPs/nt	β-APPs/nt	
0	1.00 ± 0.00	1.00 ± 0.00	1.00 ± 0.00	
wt-6	1.10 ± 0.21	1.04 ± 0.35	0.90 ± 0.21	
L392V-25	0.98 ± 0.26	0.82 ± 0.38	0.96 ± 0.52	
H163R-8	0.94 ± 0.28	1.24 ± 0.34	0.99 ± 0.32	
H163R-23	1.00 ± 0.36	1.36 ± 0.64	0.93 ± 0.40	
L286V-7	1.01 ± 0.18	0.97 ± 0.46	0.95 ± 0.70	
L286V-13	0.94 ± 0.15	1.62 ± 0.56	0.92 ± 0.40	
0	1.00 ± 0.00	1.00 ± 0.00	1.00 ± 0.00	
2/wt-9	0.75 ± 0.25	1.38 ± 0.38	0.93 ± 0.20	
2/wt-22	0.61 ± 0.18	0.64 ± 0.31	1.13 ± 0.34	
2/VG-1	0.83 ± 0.13	0.92 ± 0.44	1.15 ± 0.23	
2/VG-13	0.82 ± 0.28	1.68 ± 0.74	0.99 ± 0.37	
<i>b</i>				
Line	Aβ _{total} (ng/ml)	Aβ ₁₋₄₂ (ng/ml)	Aβ ₁₋₄₂ /Aβ _{total}	(Aβ ₁₋₄₂ /Aβ _{total})/nt
0	95.8 ± 17.2	3.86 ± 1.19	0.04 ± 0.01	1.00 ± 0.00
wt-6	96.7 ± 27.6	3.33 ± 1.00	0.03 ± 0.00	0.89 ± 0.23
L392V-25	97.4 ± 32.2	12.95 ± 7.12	0.13 ± 0.03	3.21 ± 0.61
H163R-8	154.1 ± 28.2	11.79 ± 3.14	0.08 ± 0.01	1.96 ± 0.49
H163R-23	99.8 ± 13.1	8.20 ± 0.81	0.08 ± 0.00	2.13 ± 0.48
L286V-5	79.9 ± 16.5	7.23 ± 2.66	0.09 ± 0.02	2.28 ± 0.57
L286V-7	93.2 ± 48.0	6.05 ± 1.63	0.08 ± 0.00	2.12 ± 0.41
L286V-13	135.3 ± 45.9	10.99 ± 5.24	0.08 ± 0.02	1.94 ± 0.45
0	50.2 ± 10.3	2.26 ± 0.39	0.05 ± 0.00	1.00 ± 0.00
2/wt-9	38.4 ± 11.4	2.25 ± 0.85	0.06 ± 0.01	1.26 ± 0.11
2/wt-22	40.0 ± 6.3	2.28 ± 0.50	0.06 ± 0.00	1.24 ± 0.08
2/VG-1	79.2 ± 15.7	12.56 ± 2.52	0.16 ± 0.01	3.48 ± 0.29
2/VG-13	160.5 ± 47.7	16.11 ± 1.94	0.11 ± 0.03	2.33 ± 0.59

Cells stably transfected with APP alone (0) or with PS1 wild-type (wt) or one of the indicated PS1 mutants, and lines transfected with PS2 wild-type (2/wt) or with the PS2 Volga German mutant were analyzed eight times for their steady-state levels of cellular full-length APP (fl APP), α-APPs and β-APPs by immunoprecipitation. The signals were normalized to the nontransfected cell line (nt). Data are means ± s.d. Levels of fl APP are significantly different from wild-type for the H163R-8 but not the H163R-23 clone. Compared with those of wild-type PS transfectants, levels of α-APP, in the clones H163R-23 and L286V-13 are significantly increased, but not in the clones H163R-8 and L286V-7. Compared with that in nontransfected cells, fl APP is significantly decreased by PS2 wild-type but not by PS2VG, and α-APP, is significantly decreased in the clone 2/wt-22 but not in the clone 2/wt-9. *b*, The same cell lines as in *a* were analyzed for Aβ_{total} and Aβ₁₋₄₂ production by ELISA assays. Data are means ± s.d.

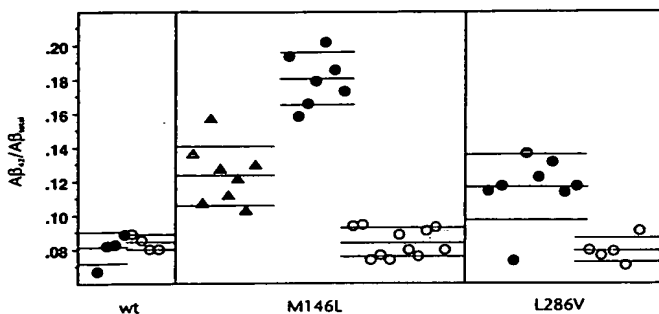


Fig. 4 $A\beta_{42}/A\beta_{total}$ ratios in the brains of double-transgenic (human *PS1* plus human *APP_{wt}*) mice (filled symbols) compared with single-transgenic littermates with the human *APP_{wt}* transgene only (open symbols). The *PS1* genotype of the double-transgenic mice is denoted below each panel. The Tg1 M146L line is indicated by triangle symbols because the $A\beta$ assays were performed at a different time.

the L286V missense mutations, which are both associated with FAD but have slightly different phenotypes (M146L FAD age of onset, 40 years; L286V FAD onset, 50 years)^{21,22}. Several different founders were obtained for each construct, bearing a range of transgene copy number up to 50–60 copies (data not shown). The expression of the *PS1* transgenes in brain was determined both by northern blotting and by western blotting using the N-terminal *PS1* polyclonal antibody, Ab14 (ref. 9).

Four independent *PS1* transgenic lines were selected for cross-breeding with the wild-type human *APP_{wt}* transgenic line Tg6209, which contains approximately 28 ± 6.1 APP copies and produces 1.6 ± 0.43 -fold more human APP than endogenous murine APP. Of the four resultant double-transgenic lines, the wild-type *PS1* line Tg195 and the L286V *PS1* line Tg198, express similar amounts of transgene-encoded mRNA (Fig. 3a, lanes 1 and 2). Because this analysis was performed with a human *PS1* cDNA probe, endogenous mouse *PS1* mRNA is not detected (Fig. 3a, lane 5), precluding an accurate estimation of net *PS1* mRNA in transgenics versus non-Tg controls. However, northern blotting with a mouse *PS1* cDNA probe indicated that human *PS1* mRNAs in the Tg195 and Tg198 lines were present at levels equal to or greater than their murine counterparts (not shown). The M146L lines Tg1 and Tg29 express *PS1* mRNA at approximately 9 times and 14 times, respectively, the level found in Tg195 and Tg198 mice (Fig. 3a, lanes 3 and 4). In accord with these mRNA results, the Tg1 and Tg29 M146L lines produced readily detectable quantities of *PS1* holoprotein (Fig. 3b, lanes 3 and 4). In the Tg195 (wild-type) and Tg198 (L286V) lines, which express *PS1* mRNA at much lower levels, the *PS1* holoprotein was barely detectable, in accord with published data on *PS1* transgenic mice⁹. However, all four *PS1* transgenic lines expressed sufficient *PS1* so that the stable ~33-kDa N-terminal proteolytic fragment of human *PS1* protein was detected and discriminated from the endogenous mouse *PS1* N-terminal product, which has a slightly slower electrophoretic mobility (Fig. 3b). Moreover, western blotting with C-terminal anti-*PS1* antibodies confirmed the presence of the complementary ~19-kDa C-terminal fragment of human *PS1* in all four transgenic lines (not shown), again as expected⁹.

Single- or double-transgenic mice were killed at 38–133 days of age (median 75.5 days), and the hippocampi were quick-frozen. The same sandwich ELISAs used for the transfected cells determined the concentration of total $A\beta$ and $A\beta_{42}$ peptides in hippocampus, a brain area strongly affected in AD. $A\beta$ levels were

measured simultaneously for the Tg29 (M146L double-transgenic), Tg198 (L286V double-transgenic) and Tg195 (wild-type double-transgenic) animals and their single-transgenic control littermates. $A\beta$ levels in the Tg1 (M146L double-transgenic) line and their single-transgenic control littermates were measured together in an independent experiment. The results showed small but significant increases in total human $A\beta$ peptides in the hippocampus of the Tg29 M146L ($P < 0.001$) and Tg198 L286V ($P < 0.01$) double-transgenic mice compared with their single-transgenic littermates. In contrast, the hippocampi from the Tg195 wild-type *PS1* double-transgenic mice showed only a small and nonsignificant increase in total $A\beta$.

Just as in the transfected cells, there was a highly significant increase in the amount of $A\beta_{42}$ in the brains of double-transgenic mice expressing M146L (Tg1) and L286V (Tg198) mutant *PS1* ($P < 0.0001$). The amount of $A\beta_{42}$ in the brains of wild-type *PS1* (Tg195) double-transgenic mice did not differ from that in the brain of the single-transgenic (*APP_{wt}*) control mice. Furthermore, the ratio of $A\beta_{42}$ to total $A\beta$ was significantly increased in the mutant but not the wild-type *PS1* double-transgenic mice ($P < 0.001$) (Fig. 4). These results were confirmed by an independent assay of $A\beta$ in the second M146L (Tg1) double-transgenic line (triangular symbols in Fig. 4). As in the transfected cells, we observed differences in the magnitude of the increase in the $A\beta_{42}/A\beta_{total}$ between the different mutations: the ratio was less in the L286V line (Tg198) than in both of the M146L lines (Tg1 and Tg29). In full agreement with the transfected cell studies, the levels of α -APP, and β -APP, in the *PS1* mutant double-transgenic brains, as measured by highly specific ELISAs (ref. 23 and K.J.-W. *et al.*, manuscript submitted), were unchanged from those in the *APP* single transgenic brains (not shown).

Discussion

Here we demonstrate that cells transfected with one of several AD-linked mutant presenilin genes all secrete significantly increased levels of $A\beta_{42}$, thus confirming the initial findings of Scheuner *et al.*⁴. This result is important in that the cells used for transfection are not derived from an individual with Alzheimer's disease, thereby unequivocally demonstrating that the observed $A\beta_{42}$ increase is directly due to the presenilin mutation and not to some other unknown confounding factor in the diseased fibroblasts. The observation that neither the double-expression system using Zeocin selection nor the overexpression of the wild-type *PS* proteins significantly changes $A\beta$ production shows that the observed effects in transfected cells are really mutation related. It is noteworthy that we extended our analysis of *PS1* mutations to the *in vivo* situation in the brains of transgenic mice. The data obtained in this independent approach are entirely consistent with the data on the transfected human cell lines. Furthermore, we observe changes in amyloidogenic APP metabolism in these mice that antedate any neuropathological evidence of neurodegeneration.

Taken together, our data strongly suggest that presenilin mutations cause a dominant gain of function, because mutant *PS* genes lead to an increase in $A\beta_{42}$ production even though the endogenous wild-type alleles are present. This increase is independent of the presenilin expression levels in the various transfected cell lines. When the $A\beta_{42}/A\beta_{total}$ ratio is normalized to that in nontransfected cells (Fig. 2, Table 1), the *PS1* wild-type and the *PS2* wild-type clones are very similar to nontransfected cells, whereas each mutant shows a highly significant increase in the $(A\beta_{42}/A\beta_{total})/\text{nontransfected}$ ratio. This increase was about

twofold for H163R and L286V, threefold for L392V and between two- and fourfold for PS2VG. It is noteworthy that the different *PS1* mutants cause highly significant differences in the degrees of $A\beta_{42}/A\beta_{total}$ elevation ($P = 0.0001$ for all L286V vs. L392V and $P = 0.0001$ for all H163R vs. L392V). Among the *PS1* mutants examined, the extent of $A\beta_{42}/A\beta_{total}$ elevation showed a crude inverse correlation with mean age of disease onset. Examination of further mutations will determine whether this relationship obtains in general for *PS1*. If it does, then additional conservative mutations in the *PS1* gene could conceivably exist that increase $A\beta_{42}$ production only very slightly, and such mutations could be risk factors for late-onset AD. The two- to threefold increase in $A\beta_{42}/A\beta_{total}$ ratio in PS2VG despite a sixfold increase in $A\beta_{42}$ is due to the simultaneous twofold increase in total $A\beta$. Our data raise the possibility of an intrinsic difference in the effects of *PS1* and *PS2* mutations on APP processing. None of the *PS1* mutants we tested had such a dramatic effect on $A\beta_{42}$ production as the PS2VG mutant (six- to eightfold increase of $A\beta_{42}$). Furthermore, only in this *PS2* mutant did we also observe a consistent and significant increase in total $A\beta$. One may speculate that mutant *PS2* affects γ -secretase processing of APP somewhat differently than does mutant *PS1*, namely, it increases the cleavage at $A\beta_{40}$ as well as that at $A\beta_{42}$. Alternatively, the nonconservative Asp to Ile substitution²⁴ in the Volga German mutation may have a more striking effect than the relatively conservative *PS1* mutations we examined. The high increase in $A\beta_{42}$ in the *PS2* mutant-transfected lines does not correlate with the relatively late age of disease onset in the Volga German kindred²⁵. However, in the brain, *PS1* and *PS2* may be differently expressed and regulated than in the transfected cell model, in which both proteins are expressed from the same promoter in all cells.

In the transgenic mouse model, we observed a small increase in total $A\beta$ peptide concentration in the brains of double-transgenic mice bearing mutant *PS1* sequences. No significant increase in total $A\beta$ peptide levels was seen in the *PS1*-transfected 293 cells. The significance of this difference remains to be determined, but might indicate that there are subtle differences in the way in which mutant *PS1* alters the γ -secretase-mediated processing of APP in brain as compared with nonneural cells. In any event, the increase in $A\beta_{42}$ production is consistently seen in all *PS1* and *PS2* mutations examined, both in transfected cells and transgenic mice, and its amount is always greater than the small and variable increase in $A\beta_{total}$ levels. These findings are entirely consistent with the recent report of a highly significant increase in the density of $A\beta_{42}$ - but not $A\beta_{40}$ -immunoreactive $A\beta$ deposits in the brains of patients bearing a *PS1* mutation²⁶.

In summary, our combined *in vitro* and *in vivo* data clearly demonstrate that FAD-linked presenilin mutations directly or indirectly alter the activity of γ -secretase but not α - or β -secretase, resulting in increased proteolysis of APP at the $A\beta_{42}$ site and heightened $A\beta_{42}$ production. The biological mechanism of this effect is presently unknown. Elucidating this process could lead to therapeutic inhibition of $A\beta_{42}$ production to prevent or slow AD, and the stable cell lines and double-transgenic mice described here should be highly useful in this quest.

Methods

***PS1* and *APP*₆₉₅ double-transfected cell lines.** Plasmids in which the *PS1* or *PS2* gene is under transcriptional control of the CMV promoter were used to stably transfect K695sw cells⁴. The expression vector pCZ was generated by cloning the CMV promoter of pCDNA3 (Invitrogen, San Diego, CA) from position 200–1175 as a *Bgl*II fragment into pZeoSV (Invitrogen) from

which the SV40 enhancer/promoter, the MCS and the SV40 pA signal (positions 2–588) had been removed by cleavage with *Bam*HI. The *PS1* expression plasmids were generated by cloning an *Eco*RI fragment of *PS1* wild-type cDNA clone CC33 (positions 1–2110 of the cDNA sequence¹⁹) into pCZ. This fragment contains the open reading frame (ORF) flanked by 190 bp of 5' UTR and 461 bp of 3' UTR. *PS2* expression plasmids were generated by cloning an *Eco*RI–*Pvu*II fragment of *PS2* wild-type cDNA (positions 1–1877 of the cDNA sequence of ref. 27) into pCZ. *PS1* and *PS2* mutant expression constructs were generated by site-directed mutagenesis of the respective wild-type cDNAs by using the nucleotide substitutions that occur in the FAD families. Stable cell lines were selected by double-resistance to Zeocin (presenilin) and G418 (*APP*). Single clones were isolated and cell extracts were analyzed for *PS* expression by immunoprecipitation.

Antibodies and immunoprecipitations. The polyclonal antibody 4627 was used to immunoprecipitate *PS1* and *PS2*. This antibody to the C-terminus of human *PS1* precipitates full-length *PS1* and *PS2* and the 18-kDa C-terminal *PS1*-fragment⁸ (M.B. Podlisny *et al.*, manuscript submitted). For immunoprecipitation with this antibody, confluent dishes were labeled for 150 min and extracts were prepared as described (M.B. Podlisny *et al.*, manuscript submitted). The following antibodies were used to analyze APP metabolites by immunoprecipitation: polyclonal antibody C7 against the last 20 residues of the APP cytoplasmic tail¹¹ precipitates N- and N' plus O'-glycosylated full-length APP as well as its C-terminal proteolytic fragments. Polyclonal antibody R1736 to residues 595–611 of APP₆₉₅ was used to precipitate α -APPs (ref. 12). This antibody recognizes an epitope that is specific for the free C-terminus of α -secretase generated APP. The polyclonal antibody sw192 (ref. 7) specifically precipitates β -secretase generated APP, carrying the Swedish mutation. The monoclonal antibody 21F12, specific for $A\beta$ and p3 peptides ending at position 42, was used as described⁴. Electrophoresis of immunoprecipitates of cell extracts or of $A\beta$ from media was done on 10–20% Tris-Tricine gels (Novex, San Diego, CA), whereas APP, precipitates were separated by electrophoresis on 10% SDS-polyacrylamide Tris-glycine gels. All quantifications were performed with a PhosphorImager 400A using Image-Quant software (Molecular Dynamics, Sunnyvale, CA).

$A\beta$ ELISA assays. Confluent 6-cm dishes were conditioned in 2 ml medium containing 10% FBS and the antibiotics used for selection for 21 h. These media were assayed by two sandwich ELISAs. First, to determine the amount of secreted total $A\beta$, monoclonal antibody 266 to $A\beta$ residues 13–28 (ref. 28) was used as capture and another monoclonal antibody, 3D6 to $A\beta$ amino acids 1–5 (K.J.-W. *et al.*, manuscript submitted) as reporter. This ELISA does not detect N-terminally truncated peptides or p3. A second aliquot of the same samples was run in an $A\beta_{42}$ -specific ELISA, using for capture 21F12, a monoclonal antibody directed to amino acids 33–42, which specifically binds $A\beta_{42}$ (ref. 14) and the same reporter (3D6) as in the total assay. This assay recognizes only $A\beta_{42}$. The sandwich ELISA for α -APPs uses monoclonal antibodies 8E5 to APP residues 444–591 and 2H3 to $A\beta$ residues 1–12. The ELISA for β -APPs uses 8E5 plus the polyclonal antibody 192 (ref. 23), specific to the free C-terminus of β -secretase-generated APP. Details of the ELISA assays are presented elsewhere (K.J.-W. *et al.*, manuscript submitted).

Statistical analysis. The data shown in Table 1 were statistically analyzed. To take day-to-day variability into account, a two-way analysis of variance (ANOVA) was used, treating the day as random effect. The analysis was carried out using log-transformations of the data and the GLM procedure in the SAS statistical software. *P* values were not corrected for multiple testing.

***PS1* transgene construction.** The wild-type *PS1* cDNA clone CC33 was mutated by site-directed mutagenesis at base pair 684 to generate the M146L missense mutation and at position 1104 to create the L286V mutation. The *Eco*RI fragment described above for the transfected lines was subcloned into the plasmid vector pZeoSV (Invitrogen), excised with *Spe*I and *Pvu*II, recombined into the *Spe*I and *Hinc*II sites of Bluescript SK2 (Stratagene, San Diego, CA), and then reexcised with *Xho*I. This 2.1-kb *Xho*I fragment was in turn cloned into the *Sal*I site of the cos.Tet vector, packaged *in vitro* (Gigapack, Stratagene), and recombinants with the appropriate orientation were identified by restriction mapping and PCR using *PS1* and PrP 3' UTR

primers. The cos.Tet vector is derived from the Syrian hamster *PrP* gene and supplies 20 kb of 5' flanking sequence, a promoter, 50 bp of a 5' UTR exon, a splice donor, a 10-kb intron, and a splice acceptor site lying upstream to the *SaII* cloning site. Downstream of the cloning site there is the 3' UTR of *PrP*, a polyadenylation signal, and 8 kb of 3' flanking sequence. The 42-kb tract of mammalian DNA cloned into the cos.Tet vector was excised from prokaryotic vector sequences using the enzyme *NotI*, gel-purified, and micro-injected by standard procedures into the fertilized oocytes of FVB/N mice. Founders were identified by Southern blot analysis of genomic DNA extracted from tail clippings using a hamster *PrP* 3' untranslated region probe. The construction of transgenic mice overexpressing human APP₆₉₅ has been described previously¹⁸. The APP transgene expressed by the Tg6209 line used in these experiments includes a MYC-epitope tag. However, identical biochemical phenotypes have been produced by tagged and untagged APP transgenes in FVB/N mice. Small tail snips from offspring of crosses between Tg6209 (wild-type human APP₆₉₅) and the PS1 lines were digested with proteinase K in 20 mM Tris, 1 mM MgCl₂, 0.5% NP-40, 0.5% Tween 20 and heat-inactivated for PCR. Primers 888 (5'-agatgagccacgcagctcc) and 910 (5'-tcacagaagataccgagact) amplified a fragment from PS1 transgenes, whereas A4-901 (5'-gacaagtatctcgagacactctgggagatgag) and A4-2070 (5'-aagaacttgtaggttgatttctgagcc) were used to detect the APP transgene.

Expression analysis in transgenic mouse brain. Total-brain RNA was prepared from transgene-positive mice (age approximately two months) by the acid-phenol method, fractionated on a 1.2% agarose gel and transferred to a Nytran Plus nylon membrane (Schleicher and Schuell, Keene, NH). The 2.1-kb human PS1 cDNA fragment was radiolabeled by random priming and used as a hybridization probe. The northern blots were washed at 0.1× SSC, 0.1% SDS at 60 °C before autoradiography. For western blot analyses, brain samples were homogenized in 9 volumes of ice-cold 0.32 M sucrose. Aliquots (12 µg) of the lysate were mixed with an equal volume of 2% SDS, electrophoresed on 12% Tris-glycine gels bracketed by the molecular weight markers "See-Blue" (Novex) and "Broad-Range" (NEB, Beverly, MA) and transferred to nitrocellulose. The N-terminal-specific anti-PS1 polyclonal antiserum 14.2 (ref. 9), raised against residues 1–25 of PS1 was used at a dilution of 1:7500, and proteins were visualized by enhanced chemiluminescence (ECL, Amersham, Arlington Heights, IL) using horseradish peroxidase (HRP)-conjugated goat anti-rabbit secondary antibody (Bio-Rad, Hercules, CA).

Aβ-peptide measurements in murine brain. Transgenic and control mice were killed by ethically approved procedures, and the hippocampi were rapidly dissected from each brain, weighed and frozen. The frozen tissue was then homogenized in either 5 volumes of homogenization buffer containing 5.0 M guanidine HCl, 50 mM Tris (pH 8.0), 20 µg/ml aprotinin, 5 mM EDTA, 10 µg/ml leupeptin (Tg29, Tg198, Tg195 and their single-transgenic littermates) or 10 volumes of homogenization buffer (Tg1 and their single-transgenic littermates), and the homogenate was assayed using the Aβ sandwich ELISAs after 10-fold dilution in 0.25% casein, PBS, pH 7.4, with protease inhibitors as in the homogenization buffer. Aβ peptide concentrations were compared between double-transgenics (with both PS1 and APP transgenes) and their single-transgenic littermates (APP transgene only) using a two-tailed Student's *t*-test.

Acknowledgments

This work was supported by National Institutes of Health grants AG 06173 and AG 12749 (to D.J.S.) and by grants from the Medical Research Council of Canada, Canadian Genetic Diseases Network — NCE Program, Alzheimer Association of Ontario, EILB Foundation, American Health Assistance Foundation and the National Institute on Aging (AG

106812) (to P.S.-H.) and the Fraternal Order of Eagles (to G.C.).

RECEIVED 23 SEPTEMBER; ACCEPTED 22 NOVEMBER 1996

1. Selkoe, D.J. Amyloid β-protein and the genetics of Alzheimer's disease. *J. Biol. Chem.* 271, 18295–18296 (1996).
2. Jarrett, J.T., Berger, E.P. & Lansbury P.T., Jr. The carboxy terminus of the beta amyloid protein is critical for the seeding of amyloid formation: Implications for the pathogenesis of Alzheimer's disease. *Biochemistry* 32, 4693–4697 (1993).
3. Scheuner, D. et al. Secreted amyloid β-protein similar to that in the senile plaques of Alzheimer's disease is increased in vivo by the presenilin 1 and 2 and APP mutations linked to familial Alzheimer's disease. *Nature Med.* 2, 864–870 (1996).
4. Yankner, B.A. New clues to Alzheimer's disease: Unraveling the roles of amyloid and tau. *Nature Med.* 2, 850–852 (1996).
5. Citron, M. et al. Inhibition of amyloid β-protein production in neural cells by the serine protease inhibitor AEBSE. *Neuron* 17, 171–179 (1996).
6. Citron, M., Teplow, D.B. & Selkoe, D.J. Generation of amyloid β-protein from its precursor is sequence specific. *Neuron* 14, 661–670 (1995).
7. Knops, J. et al. Cell-type and amyloid precursor protein-type specific inhibition of Aβ release by Bafilomycin A1, a selective inhibitor of vacuolar ATPases. *J. Biol. Chem.* 270, 2419–2422 (1995).
8. Haass, C. et al. The Swedish mutation causes early-onset Alzheimer's disease by β-secretase cleavage within the secretory pathway. *Nature Med.* 1, 1291–1296 (1995).
9. Thinakaran, G. et al. Endoproteolysis of presenilin 1 and accumulation of processed derivatives in vivo. *Neuron* 17, 181–190 (1996).
10. Walter, J. et al. The Alzheimer's disease associated presenilins are differentially phosphorylated proteins located predominantly within the endoplasmic reticulum. *Mol. Med.* (in the press).
11. Podlisny, M.B., Tolan, D. & Selkoe, D.J. Homology of the amyloid β-protein precursor in monkey and human supports a primate model for β-amyloidosis in Alzheimer's disease. *Am. J. Pathol.* 138, 1423–1435 (1991).
12. Haass, C., Hung, A.Y., Selkoe, D.J. & Teplow, D.B. Mutations associated with a locus for familial Alzheimer's disease result in alternative processing of amyloid β-protein precursor. *J. Biol. Chem.* 269, 17741–17748 (1994).
13. Haass, C. et al. Amyloid β-peptide is produced by cultured cells during normal metabolism. *Nature* 359, 322–325 (1992).
14. Citron, M. et al. Evidence that Aβ42 and Aβ40 are generated from the β-amyloid precursor protein by different protease activities. *Proc. Natl. Acad. Sci. USA* 93, 13170–13175 (1996).
15. Scott, M.R., Kohler, R., Foster, D. & Prusiner, S.B. Chimeric prion protein expression in cultured cells and transgenic mice. *Protein Sci.* 1, 986–997 (1992).
16. Prusiner, S., Scott, M., Foster, D., Westaway, D. & DeArmond, S. Transgenic studies implicate interactions between homologous PrP isoforms in scrapie prion replication. *Cell* 63, 673–686 (1990).
17. Moser, M., Colello, R.J., Pott, U. & Oesch, B. Developmental expression of the PrP gene in glial cells. *Neuron* 14, 509–517 (1995).
18. Hsiao, K.K. et al. Age-related CNS disorder and early death in transgenic FVB/N mice overexpressing Alzheimer amyloid precursor proteins. *Neuron* 15, 1203–1211 (1995).
19. Sherrington, R. et al. Cloning of a novel gene bearing missense mutations in early onset familial Alzheimer disease. *Nature* 375, 754–760 (1995).
20. Rogaeve, E.I. et al. Analysis of the 5' sequence, genomic structure and alternative splicing of the presenilin 1 gene associated with early onset Alzheimer's disease. *Genomics* (in the press).
21. Foncin, J.F. et al. Alzheimer's presenile dementia transmitted in an extended kindred. *Rev. Neurol. (Paris)* 141, 194–202 (1985).
22. Frommelt, P., Schnabel, R., Kuhne, W., Nee, L.E. & Polinsky, R.J. Familial Alzheimer disease: A large multigenerational German kindred. *Alzheimer Dis. Assoc. Disord.* 5, 36–43 (1991).
23. Seubert, P. et al. Secretion of β-amyloid precursor protein cleaved at the amino-terminus of the β-amyloid peptide. *Nature* 361, 260–263 (1993).
24. Radzicka, A. & Wolfenden, R. Comparing the polarities of the amino acids: Side chain distribution coefficients between the vapor phase, cyclohexane, 1-octanol, and neutral aqueous solution. *Biochemistry* 27, 1664–1670 (1988).
25. Sherrington, R. et al. Alzheimer's disease associated with mutations in presenilin 2: rare and variably penetrant. *Hum. Mol. Genetics* 5, 985–988 (1996).
26. Lemere, C.A. et al. The E280A presenilin 1 Alzheimer mutation produces increased Aβ42 deposition and severe cerebellar pathology. *Nature Med.* 2, 1146–1151 (1996).
27. Rogaeve, E.I. et al. Familial Alzheimer's disease in kindreds with missense mutation in a gene on chromosome 1 related to the Alzheimer's disease type 3 gene. *Nature* 376, 775–778 (1995).
28. Seubert, P. et al. Isolation and quantitation of soluble Alzheimer's β-peptide from biological fluids. *Nature* 359, 325–327 (1992).